



# Preparation of high purity biphenyl cyclooctene lignans from *Schisandra* extract by ion exchange resin catalytic transformation combined with macroporous resin separation

Chun-hui Ma, Ting-ting Liu, Lei Yang\*, Yuan-gang Zu\*\*, Feng-jian Yang, Chun-jian Zhao, Lin Zhang, Zhong-hua Zhang

Key Laboratory of Forest Plant Ecology, Ministry of Education, Northeast Forestry University, 150040 Harbin, China

## ARTICLE INFO

### Article history:

Received 7 May 2011

Accepted 12 September 2011

Available online 18 September 2011

### Keywords:

*Schisandra chinensis*

Biphenyl cyclooctene lignans

Catalytic hydrolysis

Ion exchange resin

Adsorption and desorption

Macroporous resin

## ABSTRACT

In this study, ester-bond biphenyl cyclooctene lignans were efficiently hydrolytically degraded into free biphenyl cyclooctene lignans by ion exchange resin transformation and simultaneous removal of impurities by macroporous resin. The OH-type strongly basic anion exchange resin 201 × 7 was the best one, and the dynamic hydrolysis efficiency was  $146.7 \pm 5.0\%$ . HPD5000 macroporous resin, which offered higher adsorption and desorption capacities and faster adsorption than other resins. The purity of free biphenyl cyclooctene lignans in the product increased from  $5.14 \pm 0.24\%$  to  $79.67 \pm 0.067\%$ . After dynamic catalytic transformation by 201 × 7 resin combined with purification of HPD5000 resin, the yield and the purity of free biphenyl cyclooctene lignans in the product were  $132.1 \pm 4.7\%$  and  $80.91 \pm 3.53\%$ , respectively.

Crown Copyright © 2011 Published by Elsevier B.V. All rights reserved.

## 1. Introduction

*Schisandra chinensis* Baill has a long history of medical use as a tonic, sedative and astringent agent to treat various diseases in China, Korea and Japan [1–3]. It can be used for circulatory system improvement [4], central nervous system regulation and reduction of fatigue, to increase endurance [5], for improvement of physical performance during sports [5], and for its antioxidant [6,7], anti-inflammatory [8], antitumor [9,10], anticarcinogenic [11], detoxifying, anti-hepatotoxic and anti-HIV activities [12,13]. It also can be used in the treatment of chronic coughing, asthma, heart palpitations, spontaneous sweating, insomnia, forgetfulness, spermatorrhea, diabetes [14], and cancer through its antiproliferative effects on tumor cells [15]. The major bioactive constituents of *S. chinensis* are free biphenyl cyclooctene lignans (FBCL) such as schisandrin [S], schisantherin A [SA], deoxyschisandrin [DS] and  $\gamma$ -

schisandrin [GS] [16–19]. However, the hydroxyl group in biphenyl cyclooctene lignans can easily form ester bonds with other organic acids in plants. Hydrolysis can increase the content of FBCL by transformation of ester-bond biphenyl cyclooctene lignans (EBBCL). In the hydrolysis process, cleavage of the ester bond occurs, but there are no other structural changes [20].

Homogeneous acidic or basic catalysts, such as hydrochloric acid and sodium hydroxide, are generally used for hydrolysis of esters in industry [21]. However, they cannot be recovered after use and have to be neutralized at the end of the hydrolysis reaction, resulting in secondary pollution. Ion exchange resins have high catalytic activity, can be used repeatedly, do not corrode equipment, and reduce the quantity of waste generated in catalytic reactions [22–25].

Recently, macroporous resin adsorption technology has gained popularity in pharmaceutical applications [26,27], because of its unique adsorption properties and advantages, including ideal pore structure and various surface functional groups, low operation expense, low solvent consumption, and easy regeneration [28,29], have avoided the shortcoming of liquid–liquid extraction and silica and alumina column chromatography with organic solvent [30,31].

In this report, a novel method of hydrolyzing EBBCL from *S. chinensis* extract was developed using ion exchange resin hydrolysis combined with macroporous resin purification.

\* Corresponding author at: Box 332, Northeast Forestry University, Hexing Road 26, Harbin, Heilongjiang Province, China. Tel.: +86 451 82191387; fax: +86 451 82102082.

\*\* Corresponding author at: Box 332, Northeast Forestry University, Hexing Road 26, Harbin, Heilongjiang Province, China. Tel.: +86 451 82191517; fax: +86 451 82102082.

E-mail addresses: [ylmanefu@163.com](mailto:ylmanefu@163.com) (L. Yang), [zygorl@126.com](mailto:zygorl@126.com) (Y.-g. Zu).

## 2. Materials and methods

### 2.1. Chemicals and reagents

S, SA, DS, and GS standards (98% purity) were purchased from the National Institute for the Control of Pharmaceutical and Biological Products (Beijing, China). Deionized water was prepared by a Milli-Q water purification system (Millipore, Billerica, MA). Acetonitrile and acetic acid of HPLC grade were purchased from J&K Chemical Ltd. (Beijing, China), and all of other solvents used in this study were of analytical grade from Beijing Chemical Reagents Co. (Beijing, China). Ion exchange resins SK1B and WK11 were purchased from Mitsubishi Chemical Corporation (Tokyo, Japan), others were purchased from Guangfu Fine Chemical Research Institute (Tianjin, China), and macroporous resins were purchased from Guangfu Fine Chemical Research Institute (Tianjin, China). The physical properties of resins are summarized in [Supplementary information Table S1](#) and [Table S2](#).

### 2.2. Preparation of *S. chinensis* extracts

*S. chinensis* fruits were purchased from San Keshu Trading (Heilongjiang, China) and identified by Professor Shao-quan Nie from the Key Laboratory of Forest Plant Ecology, Northeast Forestry University (Harbin, China). Dried fruits (100 g) mixed with 1000 mL of ethanol–water (80:20, v/v) solution were heated at 90 °C for 2 h and then filtered. The residue was refluxed with 800 mL of ethanol–water (80:20, v/v) for 1.5 h, filtered, then combined the twice liquid extracts and concentrated to dryness in a rotary evaporator.

### 2.3. LC–ESI–MS qualitative analysis

The structure of lignans was identified by LC–ESI–MS in order to prove that hydrolysis does not change the base core structure of biphenyl cyclooctene lignans. An Agilent 1100 series HPLC system equipped with G1312A Bin pump, G1379A degasser (Agilent, San Jose, CA, USA) and G1316A automatic column temperature control box. Chromatographic separation was performed on a HiQ sil-C18 reversed-phase column (250 mm × 4.6 mm I.D., particle size 5 μm, KYA Technologies, Tokyo, Japan). The mobile phase for elution was acetonitrile–water–acetic acid (60:40:0.1, v/v/v) at a flow

rate of 1.0 mL/min. The run time was 65 min, the injection volume was 10 μL, and the column temperature was maintained at 25 °C. An API3000 triple quadrupole mass spectrometer with a Turb Ion-Spray interface from Applied Biosystems (Carlsbad, CA) was operated in positive electrospray ionization (ESI+) mode. All mass spectra were acquired in multiple reactions monitoring mode. The analytical conditions were as follows: ion source temperature, 250 °C; nebulizing, curtain, and collision gas at 12, 10 and 6 a.u., respectively. The ion-spray voltage was 5500 V. The entrance, focusing potentials were set at 10 and 400 V, respectively. The declustering potentials were 10 V for S, 15 V for SA, 80 V for DS and G. The collision energies were 18 V for S and SA, 35 V for DS and 33 V for G. The MS parameters were manually tuned to obtain the highest response for each of the precursor/product ion combinations. Analyst software (version 1.4) installed on a Dell computer was used for data acquisition and processing.

### 2.4. HPLC–UV quantitative analysis

The quantification analysis method is according to Ma et al. [32].

### 2.5. Static tests

#### 2.5.1. Static hydrolysis tests

2.50 g of ion exchange resin (dry weight) with 50 mL of crude extract solution were shaken at 100 rpm for 12 h at 75 °C. The process was repeated three times for each set of conditions.

#### 2.5.2. Static adsorption and desorption tests

1.00 g of macroporous resin (dry weight) with 50 mL of the solution obtained after hydrolysis was shaken at 100 rpm for 8 h at 25 °C. After adsorption, the resin was washed with 50 mL of deionized water, and then static desorption was performed by shaking at 25 °C for 5 h. The process was repeated three times for each set of conditions. Adsorption isotherms on HPD5000 resin were tested at 20, 30, 40 and 50 °C, respectively.

### 2.6. Dynamic hydrolysis combined with adsorption and desorption tests

Dynamic hydrolysis combined with adsorption and desorption experiments was carried out using a fixed-bed column reactor

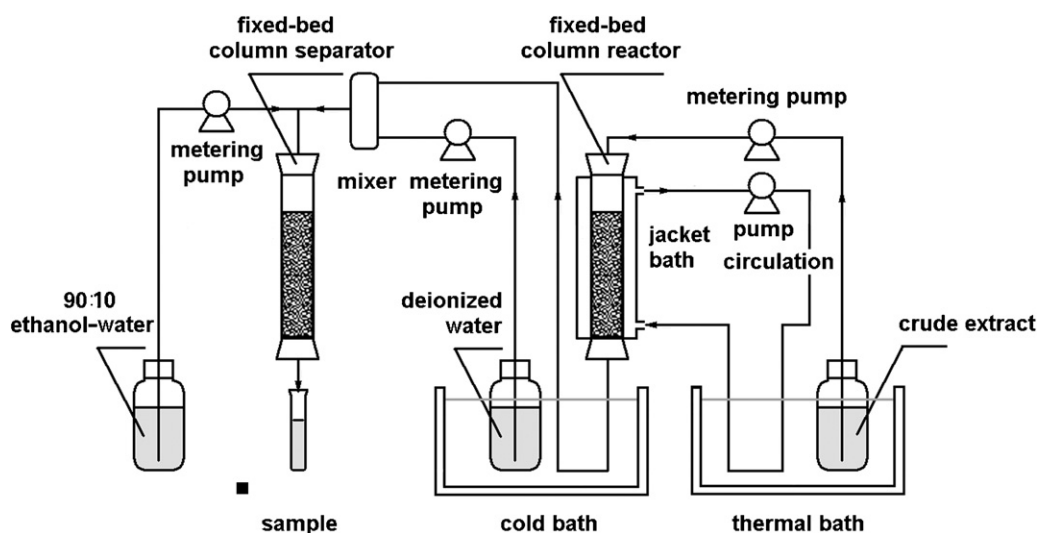


Fig. 1. Automated closed system of 201 × 7 resin hydrolysis combined with HPD5000 resin adsorption and desorption.

(20 mm × 500 mm) filled with 60.0 g of 201 × 7 resin (dry weight) connected to a fixed-bed column separator (10 mm × 250 mm) wet-packed with 24.0 g of dry HPD5000 resin (Fig. 1). The bed volumes (BV) of resin were approximately 100 mL (201 × 7) and 33 mL (HPD5000). Crude extract solution (400 mL) heated to 70 °C was pumped through the fixed-bed at 50 mL/h, which is 0.5 BV/h for 201 × 7 and 1.5 BV/h for HPD5000). The liquid after hydrolysis was mixed with cold deionized water (approximately 0 °C) (1:1) and injected into the fixed-bed column separator at 100 mL/h (3 BV/h). When the adsorption reached equilibrium, the fixed-bed column separator was washed with 100 mL of distilled water (3 BV), and then 200 mL (6 BV) of ethanol–water (90:10, v/v) at room temperature was injected into the fixed-bed column separator at 66 mL/h (2 BV/h) by a metering pump.

### 2.7. Regeneration of resins

First, the exhausted macroporous resins were washed with ethanol, then with 1 mol/L NaOH, and finally with deionized water until pH reached 7–8. The ion exchange resins were washed successively with 1 mol/L HCl and 1 mol/L NaOH (basic anion exchange resins were washed by HCl first and acidic cation exchange resins on the contrary). Finally, were washed with deionized water until pH about 7.

### 2.8. Statistical analysis

Statistical analysis of the data was performed by analysis of variance (ANOVA), and the significance of the difference between means was determined by Duncan's multiple range test ( $P < 0.05$ ) using SAS (Version 8.1, 2000; SAS Inst., Cary, NC). Values are expressed as "mean ± standard deviation".

## 3. Calculation

### 3.1. Hydrolysis efficiency evaluation

The hydrolysis efficiency was calculated using the following equation:

$$\text{Hydrolysis efficiency (\%)} = \left( \frac{C_h \times V_h}{C_0 \times V_0} \right) \times 100\% \quad (1)$$

where  $C_0$  is the initial concentration of FBCL ( $\mu\text{g/mL}$ ), which is the sum of the concentrations of S, SA, DS and GS;  $V_0$  is the volume of the initial solution (mL);  $C_h$  is the hydrolysis equilibrium concentration of FBCL ( $\mu\text{g/mL}$ ), which is the sum of the hydrolysis equilibrium concentrations of S, SA, DS and GS; and  $V_h$  is the volume of the hydrolysis equilibrium solution (mL).

### 3.2. Adsorption and desorption evaluation

The adsorption was evaluated using the following equation:

$$Q_e = (C_0 - C_e) \times V_i \times (1 - M) \times W \quad (2)$$

where  $Q_e$  is the adsorption capacity at adsorption equilibrium ( $\mu\text{g/g}$  anhydrous resin);  $C_0$  and  $C_e$  are the initial and equilibrium concentrations of FBCL, respectively ( $\mu\text{g/mL}$ );  $V_i$  is the volume of the initial sample solution (mL);  $M$  is moisture content; and  $W$  is the mass of resin (g).

Desorption was evaluated using the following equations:

$$Q_d = C_d \times V_d(1 - M) \times W \quad (3)$$

$$D (\%) = \frac{Q_d}{Q_e} \times 100\% = C_d \times V_d \times (C_0 - C_e) \times V_i \times 100\% \quad (4)$$

where  $Q_d$  is the desorption capacity after adsorption equilibrium ( $\mu\text{g/g}$  anhydrous resin);  $C_d$  is the concentration of FBCL in the desorption solution ( $\mu\text{g/mL}$ );  $V_d$  is the volume of the desorption

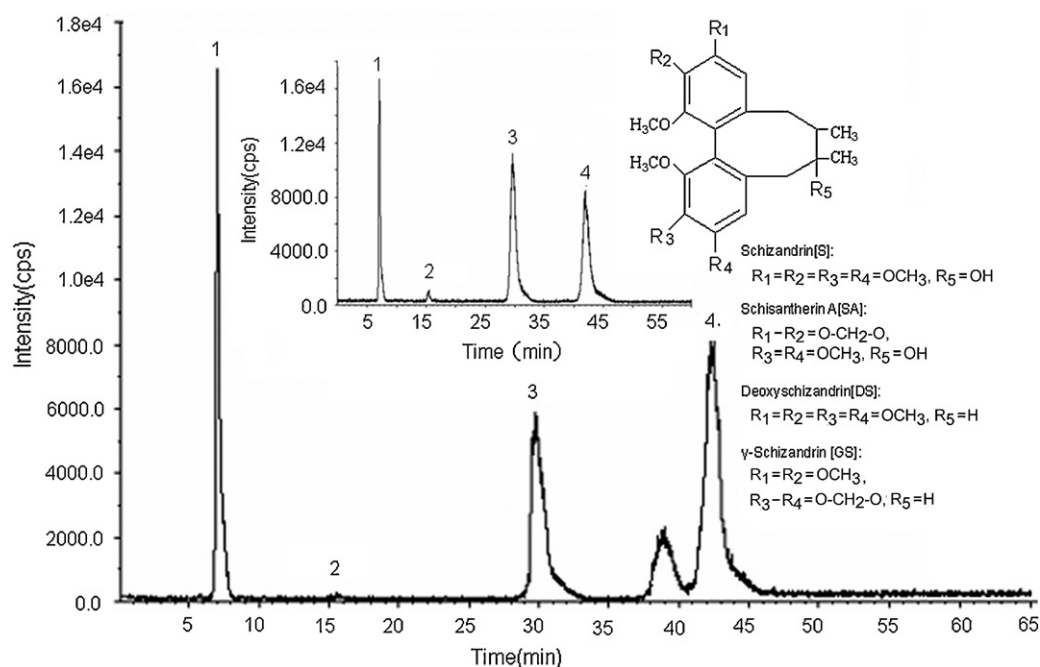


Fig. 2. Representative LC-ESI-MS chromatogram of *S. chinensis* sample. Inset: LC-ESI-MS chromatograms and molecular structures of the following four standards: (1) schizandrin [S]; (2) schisantherin A [SA]; (3) deoxyschizandrin [DS]; and (4)  $\gamma$ -schizandrin [GS].

solution (mL);  $D$  is the desorption ratio (%); and  $C_0$ ,  $C_e$ ,  $V_i$  and  $M$  are as described above.

### 3.3. Adsorption isotherms

The Langmuir adsorption model can be expressed by the following equation:

$$Q_e = Q_m \frac{C_e}{(K + C_e)} \quad (5)$$

where  $Q_e$  ( $\mu\text{g/g}$ ) is the concentration of solute per mass of adsorbent (solid phase), also known as the adsorptive capacity;  $C_e$  ( $\mu\text{g/mL}$ ) is the concentration of solute in solution (liquid phase) at equilibrium;  $K$  is the Langmuir constant; and  $Q_m$  is an empirical constant.

The Freundlich equation can be expressed as follows:

$$Q_e = KC_e^{1/n} \quad (6)$$

and in the form:

$$\ln Q_e = \ln K + \frac{1}{n} \ln C_e \quad (7)$$

where  $K$  is the Freundlich constant, which is an indicator of adsorption capacity; and  $1/n$  is an empirical constant related to the magnitude of the adsorption driving force.

### 3.4. Purity evaluation

The purity was evaluated using the following equation:

$$P = \frac{M_{\text{FBCL}}}{M_T} \times 100\% \quad (8)$$

where  $P$  is the purity of FBCL (%);  $M_{\text{FBCL}}$  is the mass of FBCL in the dry products (mg); and  $M_T$  is the total mass of dry products (mg).

## 4. Results and discussion

### 4.1. Analysis of LC-ESI-MS

According to the spectrum of *S. chinensis* standards (Fig. 2), in the positive ion mode, the first-order mass spectrum of **S** is protonated quasi-molecular ion form  $[\text{M}+\text{H}]^+$  ( $m/z$  433) and water loss ion peak  $[\text{M}+\text{H}-\text{H}_2\text{O}]^+$  ( $m/z$  415). The first-order mass spectrum of **SA** is protonated quasi-molecular ion form  $[\text{M}+\text{H}]^+$  ( $m/z$  537) and  $[\text{M}+\text{H}-\text{C}_6\text{H}_5\text{COOH}]^+$  ( $m/z$  415). The first-order mass spectrum of **DS** and **GS** are protonated quasi-molecular ion form  $[\text{M}+\text{H}]^+$  ( $m/z$  417),  $[\text{M}+\text{H}]^+$  ( $m/z$  401) broke, respectively. Compared the mass-charge-ratio ( $m/z$ ) with the data from literatures [33], the major molecular ion peaks were the initially identified, indicating that hydrolysis does not change the base core structure of biphenyl cyclooctene lignans.

### 4.2. Static process

The shaking is important to make sure that all of the resin comes into contact with the solution and the results are as accurate as possible. However, it causes resins broken under the excessive speed shaking or with a long time period. Through the pre-test, the morphology and particle size of resin were little changed at 100 rpm shaking speed within 12 h.

#### 4.2.1. Static hydrolysis of EBBCL

**4.2.1.1. Screening of ion exchange resins.** Selection of the most favorable ion exchange resin was based on the hydrolysis efficiency and the hydrolysis speed. The hydrolysis efficiencies of all the resins tested in this study are shown in Supplementary information Table

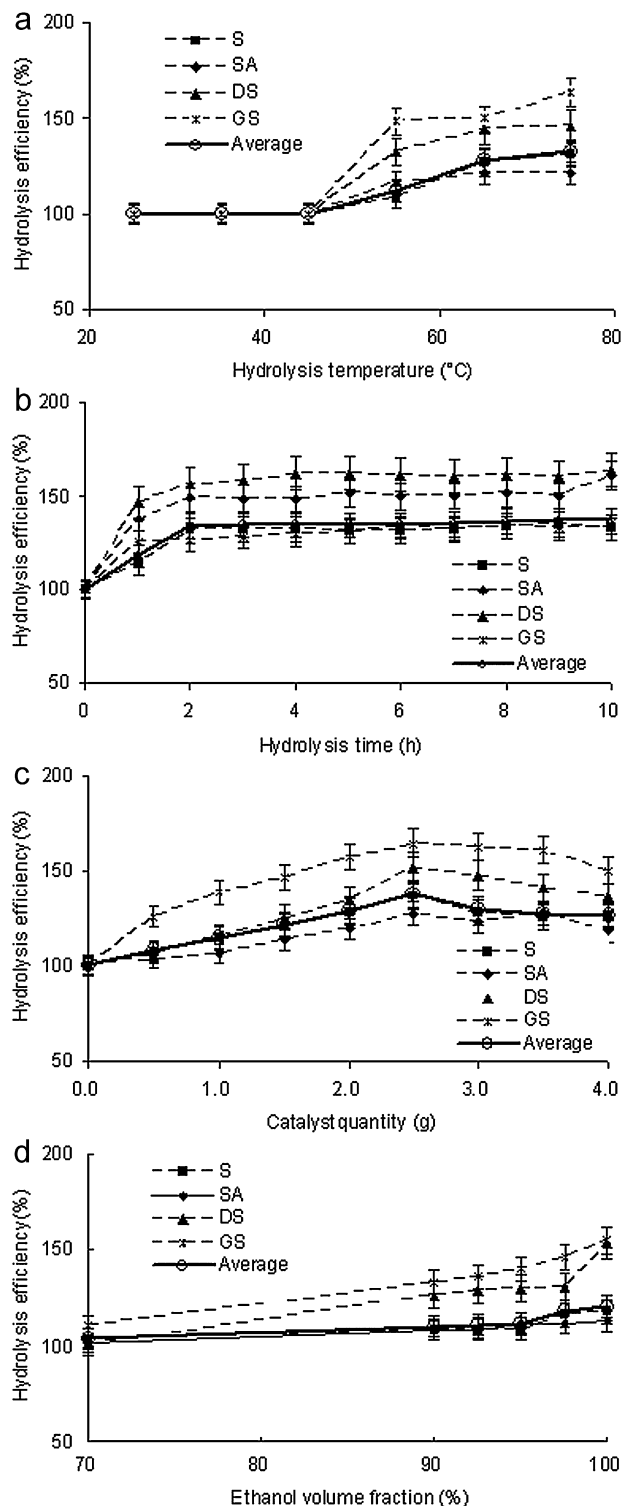


Fig. 3. Static hydrolysis testing for the effect of (a) temperature, (b) hydrolysis time, (c) catalyst quantity, and (d) ethanol volume fraction on the hydrolysis efficiency of EBBCL.

**S1.** In the test, among four types of ion exchange resins, the hydrolysis efficiency of  $201 \times 7 \text{ OH}^-$  ( $136.7 \pm 4.7\%$ ) was the highest. Hence, compared with acid hydrolysis, alkaline hydrolysis is more complete. The  $201 \times 7$  catalyst is a gel-type microporous resin. The amount of FBCL in the desorption solution was only 1.3% of crude extract solution, because the adsorption on the microporous ion

**Table 1**  
Parameters of the Langmuir and Freundlich equations.

	Temperature			
	20 °C	30 °C	40 °C	50 °C
Freundlich equation	$Q_e = 5.22C_e^{0.7554}$	$Q_e = 3.84C_e^{0.8241}$	$Q_e = 2.17C_e^{0.7677}$	$Q_e = 1.24C_e^{0.8846}$
1/n	0.7554	0.8241	0.7677	0.8846
K	5.22	3.84	2.17	1.24
R <sup>2</sup>	0.9946	0.9740	0.9530	0.8655
Langmuir equation	$Q_e = 4.2650C_e/(4.6354 + C_e)$	$Q_e = 3.0450C_e/(3.2296 + C_e)$	$Q_e = 1.8200C_e/(1.7954 + C_e)$	$Q_e = 0.9250C_e/(0.9337 + C_e)$
Q <sub>m</sub>	4.2650	3.0450	1.8200	0.9250
K	4.6354	3.2296	1.7954	0.9337
R <sup>2</sup>	0.9703	0.9575	0.9343	0.8204

exchange resin was very low. Consequently, taking into account the cost, the desorption process was not required.

**4.2.1.2. Effect of temperature.** The effect of temperature on the hydrolysis of EBBCL was studied from 25 to 75 °C with 201 × 7 resin as catalyst. The experimental results are displayed in Fig. 3(a). Below 45 °C, the hydrolysis efficiency was little changed, and 45–75 °C, it improved as the temperature increased because the hydrolysis reaction is endothermic. Ethanol is considered to be a safe and environmentally friendly organic solvent to use as the hydrolysis solvent. However, above 75 °C under normal pressure, the volatility of ethanol increases. Use of the high-pressure reaction equipment in the higher temperature hydrolysis process meant that the ethanol requirements, and therefore the cost of the process, increased and the safety decreased. In consideration of this, 75 °C was selected as the hydrolysis temperature for EBBCL hydrolysis.

**4.2.1.3. Hydrolysis kinetics.** Hydrolysis kinetic curves for EBBCL on 201 × 7 resin were obtained at 75 °C (Fig. 3(b)). The hydrolysis efficiency of EBBCL improved as the hydrolysis time increased, and reached equilibrium at about 2 h. In the first 1 h, the hydrolysis efficiency improved rapidly, and after 1 h the efficiency approached equilibrium.

**4.2.1.4. Effect of catalyst quantity.** The catalyst quantity was an important parameter in the hydrolysis reaction test. Higher catalyst loading meant the equilibrium was reached sooner because of an increase of the total number of basic sites available for the reaction (Fig. 3(c)). The appropriate amount of catalyst was 2.50 g per 50 mL of target solution. If <2.50 g of catalyst was used, the hydrolysis rate decreased, and >2.50 g of catalyst resulted in unnecessary waste.

**4.2.1.5. Effect of ethanol volume fraction on hydrolysis efficiency.** In order to investigate effect of the moisture content in solution on hydrolysis efficiency, the volume fraction of ethanol as a variable, we studied the incremental change in the static hydrolysis test. From Fig. 3(d), we can see the moisture content only a little effect on hydrolysis of DS and GS, when the ethanol volume fraction is less than 95%. However, there is little effect on average hydrolysis efficiency of EBBCL. When the ethanol volume fraction is less than 70%, the solubility of FBCL is decreased sharply, and more than 95% ethanol cause inconvenience recycling. Considering the full dissolution of FBCL and the solvent recycling issues, 90% ethanol solution was better as the hydrolysis medium for easy experimental operation.

#### 4.2.2. Static adsorption of FBCL

**4.2.2.1. Screening of macroporous resins.** The appropriate macroporous resin was selected based on the capacity of adsorption and desorption, the ratio of desorption, and the adsorption speed. The adsorption capacity and the desorption capacity of all the resins

tested in this study are shown in Supplementary information Table S2. FBCL are non-polar compounds, which meant the non-polar HPD5000 resin had highest adsorption capacity (4638 ± 261 μg/g) and higher desorption ratio (93.12 ± 3.3%) for FBCL among the resins tested. The HPD5000 resin has a bigger average pore diameter than the other resins, and this aided desorption. However, the selectivity of a single solute in multi-solute system decreased because of the increase of average pore diameter, which resulted in a high desorption ratio but low adsorption and desorption capacities [34]. Comprehensive evaluation of the adsorption capacities and desorption ratios indicated that HPD5000 resin was best among the resins for separation of FBCL, and it was used in subsequent experiments.

**4.2.2.2. Effect of ethanol volume fraction on adsorption.** Adsorption and desorption of FBCL on macroporous resin is the result of competing interactions between the intermolecular forces of adsorption on the macroporous resin and dissolution in the solvent. When intermolecular forces are dominant, FBCL adsorbs on the resin, and vice versa. Consequently, lower ethanol volume fraction makes the adsorption easier, however, if the ethanol volume fraction is too low, FBCL will co-precipitate along with other impurities, such as proteins, tannins and pigments, and adsorption does not happen easily. Therefore, the liquid after hydrolysis was mixed with deionized water in a 1:1 ratio for use in the static adsorption process.

**4.2.2.3. Adsorption and desorption kinetics curves.** The adsorption and desorption kinetics curves for FBCL on HPD5000 resin are shown in Fig. 4. The adsorption capacity of FBCL increased with the adsorption time and tended to equilibrate at about 5 h (Fig. 4(a)). In the first 3 h, the adsorption capacity increased slowly, and between 3 and 5 h it increased rapidly, while after 5 h the slope of curve indicated equilibrium was reached. The desorption ratio of FBCL increased with desorption time, and reached equilibrium at about 4 h (Fig. 4(b)).

**4.2.2.4. Adsorption isotherms.** Adsorption isotherms of FBCL on HPD5000 resin were obtained at four different temperatures (Supplementary information Fig. S). With the same initial concentration of FBCL after hydrolysis, the adsorption capacities decreased as the temperature increased from 20 to 50 °C, and the adsorption was slower than desorption, which implies that the adsorption process is exothermic. This indicates the adsorption process should be carried out at lower temperatures. Similar equilibrium isotherms were obtained for S, SA, DS and GS in Supplementary information Table S3 with initial FBCL concentrations of 58.0, 116.1, 232.3, 464.7 and 929.6 μg/mL, respectively.

The Langmuir and Freundlich parameters are summarized in Table 1. These results indicated that the adsorption process was a mono molecule layer adsorption. The correlation coefficient of

**Table 2**  
Results of the dynamic test.

The results of dynamic test	Before hydrolysis	After 201 × 7 hydrolysis	After HPD5000 purification	After 201 × 7 hydrolysis combined with HPD5000 purification
Concentration of FBCL (%)	100.0 ± 4.4	146.7 ± 5.0	90.0 ± 3.8	132.1 ± 4.7
Purity <sup>a</sup> of FBCL (%)	1.75 ± 0.05	5.14 ± 0.24	79.67 ± 0.67	80.91 ± 3.53

<sup>a</sup> Merged and concentrated the samples in a rotary evaporator under vacuum and calculated the purity of FBCL after weighting the dried solids.

Langmuir equation at 20 °C was 0.9946 the highest of all the temperatures investigated (0.9740 at 30 °C, 0.9530 at 40 °C and 0.8655 at 50 °C). The Langmuir equation at 20 °C provided the best description of the adsorption behavior of FBCL on HPD5000 resin. Therefore, 20 °C was selected as the adsorption temperature.

### 4.3. Dynamic process

#### 4.3.1. Dynamic hydrolysis

The dynamic hydrolysis efficiency for crude extract solution (200 mL, 70 °C, flow rate 0.5 × BV/h) passed through a fixed-bed column reactor filled with of 201 × 7 resin (60.0 g dry weight, BV 100 mL) was 146.7 ± 5.0%. This was slightly larger than the hydrolysis efficiency of static testing. The purity of FBCL (Table 2) in the product increased to nearly threefold compared to which of FBCL in the product before hydrolysis.

#### 4.3.2. Dynamic adsorption and desorption

Dynamic adsorption and desorption using a wet-packed (24.0 g of HPD5000 resin, BV 33 mL) fixed-bed column separator gave a FBCL concentration of 464.75 µg/mL after hydrolysis.

**4.3.2.1. Dynamic leakage curves.** When the maximum quantity of solute has adsorbed on the resin, adsorption decreases or stops, and the solute desorbs from the resin. Consequently, it is important to construct leakage curves to evaluate the quantity of resin, the volume of sample solution, and the appropriate sample flow rate. The dynamic leakage curves obtained on the HPD5000 resin were based on the volume of eluent and the flow rate. The results are shown in Fig. 5(a). At the lowest flow rate of three times the BV per hour, the best adsorption performance was obtained, which is likely because of better particle diffusion in the sample solutions. However, the lower flow rate increased the experimental time. Despite this, three times the BV per hour was chosen as the most appropriate sample flow rate for further experiments. Under this condition, the volume of sample solution was approximately 13 times the BV.

**4.3.2.2. Dynamic desorption curves.** Dynamic desorption curves on HPD5000 resin were obtained based on the volume and flow rate of the desorption solution. Ethanol–water solutions with different volume fractions (50:50, 70:30, 90:10, v/v) were used for the desorption tests. As the ethanol volume fraction increased, the desorption ratio increased rapidly (Fig. 5(b)). To ensure efficiency and economy of the process, ethanol–water (90:10, v/v) solution was selected as the desorption solution and used in the dynamic desorption experiment.

The flow rates investigated in this test were 2, 3 and 4 BV/h. At the flow rate of 2 BV/h, FBCL was totally desorbed with a solvent volume of 6 BV (Fig. 5(c)). By comparison, at the flow rates of 3 and 4 BV/h, FBCL was totally desorbed with a solvent volume of 7 and 8 BV, respectively. These results indicate that the lower desorption flow rate produced the most concentrated product among the flow rates tested. Therefore, this flow rate is better for the adsorption in terms of lower solvent use and high efficiency.

The dynamic adsorption and desorption results and optimized parameters can be summarized as follows. For adsorption, the concentration of FBCL in the sample solution after hydrolysis was 464.75 µg/mL. The processing volume was 430 mL (13 BV), and the flow rate was 3 BV/h. And then be washed with 3 BV deionized water at a flow rate of 3 BV/h. For desorption, the elution solvent was ethanol–water (90:10, v/v) 200 mL (6 BV) at a flow rate of 2 BV/h. Samples after purification by HPD5000 resin were combined, concentrated in a rotary evaporator, and dried under vacuum, the purity of FBCL increased 15.5-fold from 5.14% to 79.67%, and the FBCL recovery was 90.04% (Table 2).

### 4.4. Results of dynamic hydrolysis combined with dynamic adsorption and desorption test

Dynamic hydrolysis combined with dynamic adsorption and desorption test was conducted under the conditions shown in Section 2.6 with 201 × 7 and HPD5000 resins. The yield and purity of FBCL (Table 2) in the product were 132.1 ± 4.7% and 80.91 ± 3.53%, respectively.

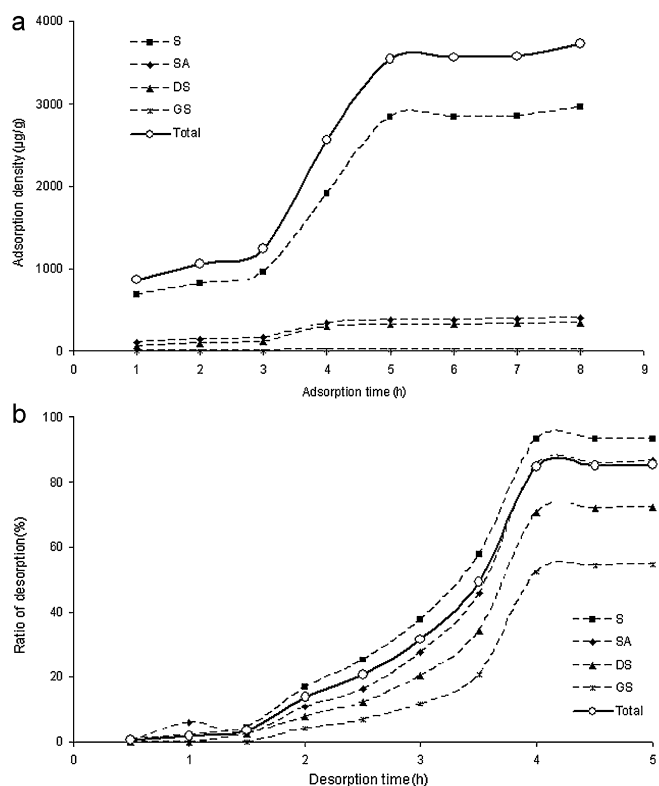


**Fig. 4.** The adsorption (a) and desorption (b) kinetic curves for FBCL on HPD5000 resin.

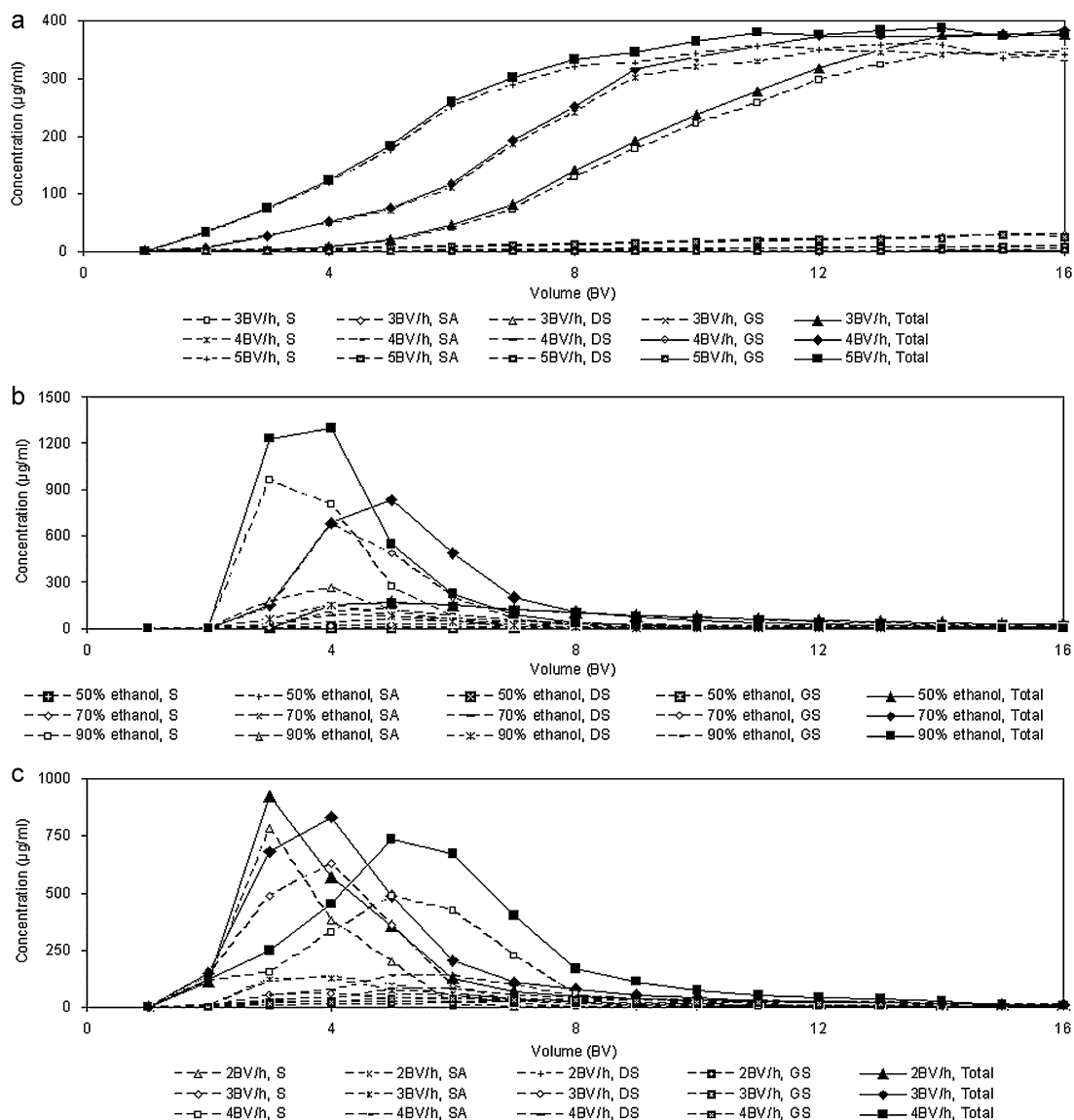


**Fig. 5.** Leakage curves for (a) with different current velocity, (b) dynamic desorption curves with different ethanol volume fractions, and (c) the dynamic desorption curve with different current velocity.

#### 4.5. Reuse of resins in continuous processes

The exhausted resins were regenerated as described in Section 2.7. After the resins had been regenerated 10 times, their hydrolysis densities and adsorption capacities had decreased to 86.26% and 79.34% of their initial values. This indicates that the regenerated resin could be used in a continuous process for FBCL purification.

## 5. Conclusions

In this study, an efficient automated and continuous system for purifying FBCL using ion exchange resin and macroporous resin was developed. The catalytic hydrolysis of EBBCL, simultaneous removal of impurities, and production of FBCL was readily achieved in a simple and economic manner. The optimum dynamic hydrolysis combined with adsorption and desorption was performed with crude solution (400 mL) pumped through a fixed-bed column reactor at a flow rate of 50 mL/h. The fixed-bed column separator was then washed with deionized water at a flow rate of 3 BV/h, and ethanol–water (90:10, v/v) at 2 BV/h. The yield and the purity of FBCL in the product were  $132.1 \pm 4.7\%$  and  $80.91 \pm 3.53\%$ ,

respectively. This method could be used for efficient purification of FBCL from *S. chinensis*. Satisfactory regeneration of the  $201 \times 7$  and HPD5000 resins indicates that the process could be applied for industrial purification of plant constituents.

## Acknowledgements

The authors acknowledge the financial supports by the Fundamental Research Funds for the Central Universities (Grant no. DL09BB48), the National Key Technology R&D Program (Grant no. 2006BAD18B 04) and China–Germany Inter-Governmental Cooperation Program (Grant no. CHN 3/028).

## Appendix A. Supplementary data

Supplementary data associated with this article can be found, in the online version, at doi:10.1016/j.jchromb.2011.09.022.

## References

- [1] J.Y. Park, H.K. Shin, Y.J. Lee, Y.W. Choi, S.S. Bae, C.D. Kim, *Ethnopharmacology* 121 (2009) 69.
- [2] G.T. Chang, S.K. Kang, J.H. Kim, K.H. Chung, Y.C. Chang, C.H. Kim, *Ethnopharmacology* 102 (2005) 430.
- [3] C.G. Wang, *Basic Theory Traditional Chinese Medicine*, Shanghai of TCM Press, Shanghai, 2002.
- [4] L. Opletal, M. Krenkova, P. Havlickova, *Ceska a Slovenska Farmacie* 50 (2001) 173.
- [5] J.Y. Peng, G.R. Fan, L.P. Qu, X. Zhou, Y.T. Wu, *J. Chromatogr. A* 1082 (2005) 203.
- [6] P.Y. Chiu, D.H.F. Mak, M.K.T. Poon, K.M. Ko, *Plant. Med.* 68 (2002) 951.
- [7] K.M. Ko, Y.H. Lam Brian, *Mol. Cell. Biochem.* 238 (2002) 181.
- [8] L.Y. Guo, T.M. Hung, K.H. Bae, E.M. Shin, H.Y. Zhou, Y.N. Hong, S.S. Kang, H.P. Kim, Y.S. Kim, *Eur. J. Pharmacol.* 591 (2008) 293.
- [9] X.X. Deng, X.H. Chen, R. Yin, Z.D. Shen, L. Qiao, K.S. Bi, *Pharmaceut. Biomed. Anal.* 46 (2008) 121.
- [10] D.F. Chen, S.X. Zhang, M. Kozuka, Q.Z. Sun, J. Feng, Q. Wang, T. Mukainaka, Y. Nobukuni, H. Tokuda, H. Nishino, H.K. Wang, Morris-Natschke, L. Susan, K.H. Lee, *Nat. Prod.* 65 (2002) 1242.
- [11] M. Fu, Z.H. Sun, M. Zong, X.P. He, H.C. Zuo, Z.P. Xie, *Acta Pharmacol.* 29 (2008) 891.
- [12] B. Bharate Sandip, *Med. Aromatic Plant Sci.* 25 (2003) 427.
- [13] D.F. Chen, S.X. Zhang, B.N. Wang, P. Zhou, L.M. Wang, Cosentino, K.H. Lee, *Nat. Prod.* 59 (1996) 1066.
- [14] J.N. Wu, *An illustrated Chinese Materia Medica*, Oxford University Press, New York, 2005, p. 574.
- [15] H.Y. Min, E.J. Park, J.Y. Hong, Y.J. Kang, S.J. Kim, H.J. Chung, E.R. Woo, T.M. Hung, U.J. Youn, Y.S. Kim, S.S. Kang, K. Baec, S.K. Lee, *Bioorg. Med. Chem. Lett.* 18 (2008) 523.
- [16] Y.H. Kuo, L.M. Kuo, C.F. Chen, *Org. Chem.* 62 (1997) 3242.
- [17] Y.G. Chen, G.W. Qin, Y.Y. Xie, K.F. Cheng, Z.W. Lin, H.D. Sun, Y.H. Kang, B.H. Han, *Asian J. Nat. Prod. Res.* 1 (1998) 125.
- [18] Y.W. Choi, S. Takamatsu, S.I. Khan, P.V. Srinivas, D. Ferreira, J. Zhao, I.A. Khan, *Nat. Prod.* 69 (2006) 356.
- [19] A. Panossian, G. Wikman, *Ethnopharmacology* 118 (2008) 183.
- [20] Y.G. Chen, G.W. Qin, Y.Y. Xie, *Chem. World* 07 (2001) 380.
- [21] S.K. Naomi, H. Hiroki, K. Homare, T. Takuji, F. Takuya, Y. Toshikuni, *Bioresour. Technol.* 98 (2007) 416.
- [22] M.K. Basu, D.C. Sarkar, B.C. Ranu, *Synth. Commun.* 19 (1989) 627.
- [23] H. Samelson, L.P. Hammett, *Am. Chem. Soc.* 78 (1956) 524.
- [24] Y. Miyazaki, G. Kura, H. Tsuzuki, H. Sakashita, *J. Chem. Soc., Faraday Trans.* 92 (1996) 3587.
- [25] Z.W. Xu, W.M. Zhang, L. Lv, B.C. Pan, P. Lan, Q.X. Zhang, *Environ. Sci. Technol.* 44 (2010) 3130.
- [26] Q.H. Cao, W.J. Qu, Y.X. Deng, *J. Chin. Mater. Med.* 29 (2004) 225.
- [27] B.Q. Fu, J. Liu, H. Li, L. Li, S.C. Lee Frank, X.R. Wang, *J. Chromatogr. A* 1089 (2005) 18.
- [28] M. Gao, W. Huang, C.Z. Liu, *J. Chromatogr. B* 858 (2007) 22.
- [29] Z.Y. Lou, H. Zhang, C.G. Gong, Z.Y. Zhu, L. Zhao, Y.J. Xu, B. Wang, G.Q. Zhang, *Rapid Commun. Mass Spectrom.* 23 (2009) 831.
- [30] C.-S. Liu, S.-D. Fang, M.-F. Huang, Y.-L. Kao, J.-S. Hsu, *J. Sci. Sin. Ser. A* 21 (1978) 483.
- [31] L. Březinova, H. Vlašínova, L. Havel, O. Humpa, J. Slanina, *J. Chromatogr. A* 24 (2010) 954.
- [32] C.H. Ma, T.T. Liu, L. Yang, Y.G. Zu, S.Y. Wang, R.R. Zhang, *Anal. Chim. Acta* 689 (2011) 110.
- [33] X. Huang, F.R. Song, Z.Q. Liu, S.Y. Liu, *Acta Chim. Sin.* 66 (2008) 1059.
- [34] G.T. Jia, X.Y. Lu, *J. Chromatogr. A* 1193 (2008) 136.